ISSN 1054-660X, Laser Physics, 2007, Vol. 17, No. 11, pp. 1–6.

Concept Study of a 100-PW Femtosecond Laser Based on Laser Ceramics Doped with Chromium Ions

E. A. Khazanov and A. M. Sergeev

Institute of Applied Physics, Russian Academy of Sciences, ul. Ulianova 46, Nizhni Novgorod, 603950 Russia

e-mail:

Received June 20, 2007

Abstract—A new concept of a superpowerful femtosecond laser based on CPA in polycrystalline chromium doped ceramics (Cr:YAG, Cr:YSGG, etc.) pumped by a Nd:glass laser is proposed. In contrast to amplifiers in available petawatt laser systems (neodymium glass, titanium-doped sapphire, and parametric amplifiers with a DKDP crystal), these ceramics combine three key favorable properties: a large gain bandwidth to amplify chirped pulses with less than 20-fs durations, a wide aperture to amplify chirped pulses to the multikilojoule level, and a high conversion efficiency of narrowband Nd:glass laser pulses into chirped pulses. These properties open up the opportunity to create a unique laser with a peak power of 100 PW at a 10-kJ pump power.

PACS numbers: 06.60.Jn, 42.70.Hj, 42.60.Ov, 42.55.Px, Rz

DOI: 10.1134/S1054660X0711@@@@

1. INTRODUCTION

Petawatt-level laser pulses make it possible to experimentally investigate highly nonlinear processes in atomic, molecular, plasma, and solid-state physics and to access previously unexplored states of matter. The petawatt laser power was achieved as early as 1997 [1], based on chirped-pulse amplification in Nd:glass. Until now, an additional four laboratories have reported petawatt-level laser systems [2–5]. Many laboratories are pursuing this power level [6–14], but any further increase to 10 PW or more is limited by the following principal conditions.

All devices and projects now available may be classified into three types, according to the gain medium they employ: (1) neodymium glass [1–3, 8–12], (2) titanium-sapphire [4, 13], and (3) optical parametric amplifiers with KDP and DKDP crystals [5–7, 14] (see Table 1). In all three types, energy (in the form of population inversion) is stored in neodymium ions in glass. In the first case, this energy is directly converted into the energy of a chirped pulse that is then compressed. In the second and third cases, the stored energy is converted into the energy of a narrowband nanosecond pulse, which, upon second-harmonic conversion, serves as the pump for chirped-pulse amplifiers. This pump either provides population inversion in a Ti:Sa crystal or is parametrically converted into chirped pulses in the nonlinear crystal.

Peak power is determined by the duration and energy of the compressed pulses. Maximum energy is achieved in glass-based lasers, because energy that has been stored as population inversion is directly converted into a chirped pulse. However, the narrow band-

Table 1. Comparison of known petawatt laser concepts and the proposed concept. Symbols "+", "–", and "0" denote advantages, disadvantages, and the average in comparison with other concepts

	1		2		3		4	
Gain medium	Nd : glass		Ti : sapphire		DKDP		Cr : YAG ceramic	
Energy source	Nd : glass		Nd : glass		Nd : glass		Nd : glass	
Pump	no	(+)	2ω Nd	(–)	2ω Nd	(–)	1ω Nd	(0)
Pump duration, ns	no	(+)	>10	(0)	1	(–)	>10	(0)
Amplifier aperture, cm	40	(0)	8	(–)	40	(0)	>50	(+)
Minimum duration, fs	500	(–)	25	(+)	25	(+)	25	(+)
Efficiency (1ω Nd ⟶ fs), %	80	(+)	15	(–)	10	(–)	25	(0)
Number of PWs from a 1-kJ 1ω Nd	1.6(1.5)*		6(1.5)*		4		10	
Maximum power obtained, PW	1.36 [1]		0.84 [4]		0.56 [4]		–	

* Optical breakdown of diffraction gratings and Ti:sapphire crystals limit maximum power to 1.5 PW.

Table 2. Parameter of Cr:YAG crystal

Parameter	Dimension	Value
ground-state absorption cross section @1064 nm, σ_{gs}	10^{-19} cm^2	70 [27]
		60 [28] (T = 10 K)
		37–77 (29)
		50 [30–32]
		38–51 [33]
		30 [24]
		25 [35]
		8.7 [36]
laser transition cross section, σ_{ias}	10^{-19} cm^2	7–8 [30, 31]
		3.5 [28]
		3.3 [37]
		2.2–3.3 [38]
		2 [39]
		0.69–1.5 [40]
excited-state absorption crosssection @1064 nm, σ_{es}	10^{-19} cm^2	20 [27]
		8 [29]
		5 [30, 31]
		3 [35]
		2.2 [36]
		2 [34]
		<0.2 [33]
excited-state absorption cross section @1450 nm, σ_{las_ab}	10^{-19} cm^2	4–5 [30, 31]
		0.8 [39]
		0.7 [38]
		0.05–0.82 [40]
excited-state lifetime @300 K, τ	μs	4.1
excited-state lifetime @77 K, τ_{77}	μs	25
lifetime at level after ESA, τ*	μs	0.5 [27]
		0.1 [30]

width of Nd glasses typically restricts the compressed-pulse duration to about 500 fs.

Ti:sapphire lasers have a large-gain bandwidth, allowing pulse compression up to 10–20 fs. At the same time, available crystal growth technologies can produce Ti:sapphire crystals with an aperture of no more than 10 cm. When attempting to overcome the petawatt energy level, such a small aperture will limit the chirped-pulse energy due to optical breakdown and self-focusing.

Parametric amplifiers are free of the above disadvantages. Current nonlinear KDP and DKDP crystals have an aperture of 40 cm or more and the gain bandwidth of the DKDP corresponds to a 10–20-fs duration of the amplified pulse. At the same time, in parametric amplifiers, the energy conversion efficiency of a Nd:laser monopulse into a chirped pulse is typically only at the level of 10%. Also, parametric amplifiers require very-short (about 1 ns) pump pulse.

Thus, in existing approaches to petawatt and multi-petawatt lasers, the peak power is limited either by the bandwidth (neodymium ion lasers), the crystal aperture (Ti:sapphire lasers), or the efficiency of the energy conversion from a pump wave into a signal wave (lasers with optical parametric amplifiers).

In this paper, we introduce a new concept, which is based on the use of polycrystalline chromium-doped ceramics as an active medium. Pumping may be either by flash lamps or by the first harmonic of a nanosecond Nd:glass laser. In the former case, the advantages are evident, but there is also the significant drawback of the short lifetime of chromium ions (e.g., 4.1 μs at room temperature and 25 μs at liquid-nitrogen temperature in Cr:YAG). This will require a greater (as compared to Nd:glass lasers) number of flash lamps, since the energy limit that the lamps can withstand is proportional to the root of the current pulse duration. The first-harmonic pump is free of this disadvantage, so we will concentrate on this option below.

In contrast to the above-mentioned laser media, polycrystalline chromium-doped ceramics such as Cr:YAG, Cr:YSGG, etc., simultaneously have a large bandwidth, a wide aperture, and a high conversion efficiency of narrowband radiation of the first harmonic of Nd:glass lasers. These properties open up the opportunity to create a unique laser that would produce peak power unattainable, in principle, by other techniques.

2. POLYCRYSTALLINE CR:YAG CERAMICS

Polycrystalline Cr:YAG ceramics combine the advantages of laser ceramics and Cr:YAG single crystals. Below, we discuss these advantages.

Polycrystalline laser ceramic, a new optical material, has recently found wide application. Owing to the flexibility of its fabrication technology, ceramics can be made of various cubic crystals with different ions. In some cases, it is simply impossible to grow a corresponding single crystal. Many properties of laser ceramics, such as absorption and emission spectra, transition cross section, upper-level lifetime, temperature dependence of the refractive index, breakdown threshold, chemical stability, etc., are close to those of single crystals. At the same time, ceramics are highly competitive with laser glasses in some parameters: the possibility of making a large aperture (up to 1 m), controllable activator distribution, high critical concentration of the activator, possible control of the physical, chemical and spectroscopic characteristics, perfect optical quality, and low cost. Therefore, ceramic materials have a unique set of properties that neither single crystals nor glasses possess.

The power of cw Nd:YAG ceramic lasers reached 1.5 kW in 2002 [15] and is now approaching 100 kW. In ceramic lasers, not only cw generation, but also q-switched [16, 17], pico-, and femtosecond generation regimes [18, 19] were demonstrated. Lasing at different wavelengths, including 1.3 micron, were obtained in Nd:YAG ceramics [20]. To the best of our knowledge, no Cr:YAG ceramic laser has been reported thus far, though Cr:YAG ceramic elements have been used as passive q-switchers [17, 21].

Since the late 1980s [22], Cr:YAG single crystals have attracted much attention due to their unique properties that allow their use as q-switchers for neodymium lasers as well as active elements. Cr:YAG is widely used for the creation of tunable and femtosecond lasers in the near-IR range [23]. Passive q-switching in Cr:YAG lasers has been achieved not only by Kerr lens mode-locking, but by synchronous pumping [24] and semiconductor saturable absorber [25] as well. By using dispersion-compensating double-chirped mirrors, 18-fs pulses have been generated [26].

The Cr:YAG crystal has a number of peculiarities that considerably affect the processes of pumping, amplification, and generation. These include, first, a large pump absorption cross section and a small gain cross section (see Table 2); second, excited-state absorption (ESA) of pump and laser radiation (see Fig. 1); third, saturation anisotropy associated with selective excitation of chromium ions in three tetrahedral sites that are distorted along the three orthogonal crystallographic axes; and fourth, a high ratio between radiative and nonradiative lifetimes of the upper-laser level. The latter feature leads to a reduced lifetime, which is important for the cw pump, but makes no significant difference for amplifiers pumped by nanosecond pulses.

3. LARGE CROSS SECTION OF PUMP ABSORPTION AND ESA

A small gain cross section of Cr:YAG makes it difficult to create single amplifiers with a high gain coefficient. Preamplification stages (from nJ to a few J) can be careated as an optical parametric amplifier based on a BBO crystal. When pumped by the second harmonic of a neodymium laser, this crystal has ultra-broadband phase matching in the range of 800–900 nm [41], and, in this case, an idler wave falls into the gain bandwidth of Cr:YAG. For the next stages, multiple-pass amplifiers can be used that do not require high-gain single-pass coefficients.

To create power amplifiers from 10 J to kilojoules, a more difficult problem is that σ_{gs} is large, rather than σ_{gs} being small, and, in particular, that $\sigma_{las} \ll \sigma_{gs}$ and, hence, $E_{slas} \gg E_{spump}$. (Note that the ratio of these cross sections is inverse to that in the Ti:sapphire crystal, see Table 3). The values of σ_{gs} (and, therefore, $E_{spump} = h\nu/\sigma_{gs}$) reported in the literature vary by more than one order of magnitude (see Tables 2 and 3). In the creation of a multipetawatt Cr:YAG laser, most problems will come at maximum σ_{gs}; therefore, here and below, we shall assume the largest $\sigma_{gs} = 70 \times 10^{-19}$ cm^2 in accordance with [27].

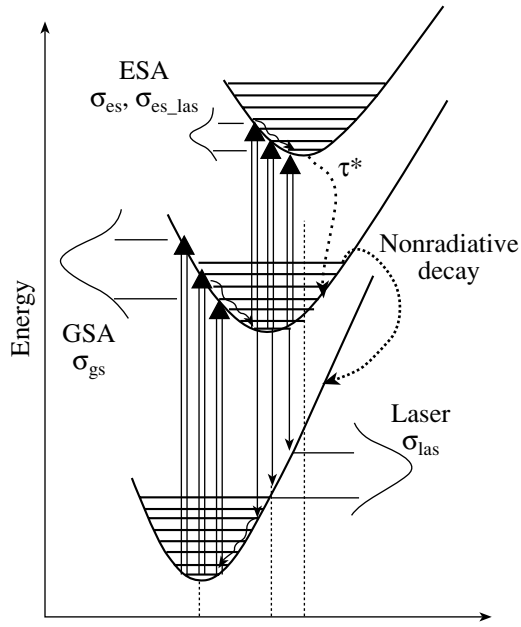

Fig. 1. Schematic diagram of Cr:YAG levels.

Because of $\sigma_{las} \ll \sigma_{gs}$ and a large value of σ_{gs}, a highly efficient Cr:YAG amplifier will require (1) a high area ratio of pump beams and amplified wave $S_{slas} \ll S_{spump}$ and (2) a pump energy density exceeding E_{spump}, which requires the suppression of ESA. The first requirement can be met by choosing the appropriate geometry of the active medium—either a slab, a side-pumped rod, or several disks (Fig. 2).

The values of the ESA cross section of pump radiation σ_{es} and laser radiation σ_{las_ab} reported in publications vary even more than σ_{gs}. All literature data are summarized in Table 2. Most authors mention large values for the ESA of pump radiation [27, 29–31, 35, 42, 43]. On the contrary, in [33], the authors claim that the ESA of the pump radiation is negligible. Measurements of σ_{las_ab} in all publications are indirect and also extremely varied (see Table 2). The ratio $\sigma_{las\_ab}/\sigma_{las}$ varies less, but needs further investigation in any case. If we assume that $\sigma_{las\_ab}/\sigma_{las} = 0.3$, the effective stored energy decreases by about 30%, so that the efficiency of the laser amplifier decreases by 30% as well.

In the case of the ESA of the pump beam, estimations show that, at a pump energy density five times higher than E_{spump}, the pump energy losses by ESA will be 20–30% (we assume the worst data from [27]). For a disk with an 80×40 cm^2 aperture at two-side pumping, this value corresponds to a pump energy of 830 J.

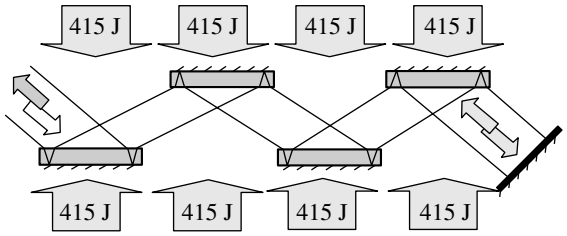

Fig. 2. Amplifier geometry (example).

To increase this energy at the same ESA-induced energy loss level, the following measures seem promising. First, temporal matching between the pump pulse and the amplified wave will decrease the population of the upper-laser level. Second, it is advisable to arrange several passes of the amplified light if the pump is delivered between the passes, for instance, as a pump-pulse duration equal to the total time of all passes of the signal through the amplifier. As a result, at the same power losses by ESA, the pump energy will be increased by a number of times equal to the number of passes. Moreover, Cr:YAG ceramic active elements may be placed directly in the beam path of multiple-pass Nd:glass amplifiers.

In addition, a decrease of σ_{gs} in ceramics may be expected due to saturation anisotropy in Cr:YAG, because the orientation of the crystallographic axes in each grain is random. An accurate model of the absorption in Cr:YAG ceramic, which would take into account the anisotropy of the absorption saturation, has not been developed. Estimations can be made by using the well-known model for an arbitrarily oriented single crystal [44]. If we assume an orientation with the laser wave field directed along the diagonal of the cubic lattice, we can show that the absorption is described by the Frantz–Nodvik formula [45] at the effective cross section of $\sigma_{gs}/3$. For the [001] orientation, the effective cross section will vary from σ_{gs} to $\sigma_{gs}/2$, depending on the polarization direction. In the stationary case, averaging the expressions presented in [46] over all possible orientations results in a twofold decrease in σ_{gs}. The question of precisely how much the decrease in σ_{gs} (and, consequently, an increase in E_{spump} in Cr:YAG ceramics) needs further investigation. But, in any case, the decrease in σ_{gs} considerably lowers the above limitations. Note that the cross section of σ_{es} will decrease by the same numbers as σ_{gs}. Also, further investigation should be done to measure the laser and ESA cross sections for orthogonally polarized beams [33, 35, 39].

4. CHROMIUM IONS IN MATRICES OF OTHER CUBIC CRYSTALS

The YAG crystal is not the only crystal in which chromium ions have a broadband emission spectrum. A large number of garnets are available and some of them have a set of properties that are not inferior to those of YAG (see Table 3). For example, the effect of ESA is almost completely excluded in the Cr:YSGG crystal, for which $\sigma_{gs} = 11\sigma_{es}$ [27]. In addition, the absolute value of σ_{gs} in Cr:YSGG is much lower than in Cr:YAG, while the value of σ_{las} is higher. This combination of parameters makes Cr:YSGG a very promising laser material. For instance, in a disk with an aperture of 80×40 cm^2, the energy losses of about 20–30% will occur at a pump energy of 3.6 kJ. Note that, in contrast to YAG, there is almost no selective excitation of chromium ions in YSGG [47].

Table 3. Parameters of various Cr^{4+}-doped garnets: λ_{max} is a wavelength with a maximum gain cross section, $\Delta\lambda$ is the gain bandwidth. For Cr^{4+} : YAG parameters see also Table 2

Lattice	Abbreviation	λ_{max}, nm [37]	$\Delta\lambda$, nm [37]	τ, μs [37]	σ_{las}, 10^{-19} cm^2	σ_{gs}, 10^{-19} cm^2 [27]	σ_{es}, 10^{-19} cm^2 [27]
$Lu_3Al_5O_{12}$	LAG	1370	232	5.6	3.4		
$Y_3Al_5O_{12}$	YAG	1378	224	4.1	3.3	70	20
$Y_3Sc_xAl_{5-x}O_{12}$	YSAG ($x = 0.22$)	1397	233	4.1	3.1		
	YSAG ($x = 0.48$)	1407	237	3.3	3.3		
	YSAG ($x = 1.20$)	1468	268	2.0	4.1		
	YSAG ($x = 1.50$)	1508	303	1.5	4.5		
	YSAG ($x = 1.72$)	1593	298	1.4			
$Y_3Ga_5O_{12}$	YGG	1456	238	1.9	4.3		
$Gd_3Ga_5O_{12}$	GGG	1442	231	2.2	4.5	58	13
$Gd_3Sc_2Al_3O_{12}$	GSAG	1599	276	1.7	4.8		
$Y_3Sc_2Ga_3O_{12}$	YSGG	1561	279	1.3	5.2	45	4
$Gd_3Sc_2Ga_3O_{12}$	GSGG	1582	299	2.0	3.6		
	Ti:sapphire	760	250	3.1	4.5	0.2–0.5	

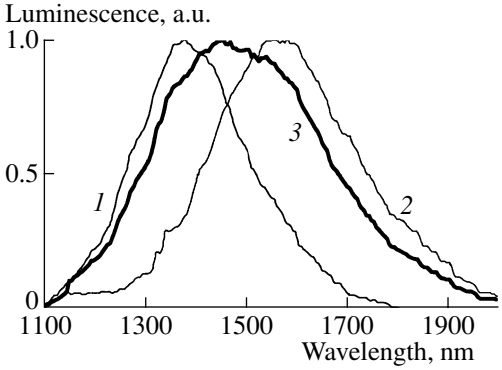

Fig. 3. Emission spectra of YAG (1), YSGG (2) crystals [37], and the total spectrum (3).

The central wavelength of the laser transition is different in different crystals (see Table 3). Therefore, one may use combinations of different crystals to additionally broaden the gain bandwidth, by analogy, with amplification of broadband pulses in different types of Nd:glass. The total gain bandwidth of Cr:YAG and Cr:YSGG is almost two times broader than in YAG (Fig. 3).

5. EXAMPLE OF A 100-PETAWATT LASER

As an example, we present estimations for the maximum energy parameters of a femtosecond Cr:YAG ceramic laser pumped by the high-power laser fusion facility "Luch" [48] producing a 3.3-kJ pulse energy at 1053 nm in one of its channel. When four Cr:YAG disks with a 80×40 cm^2 aperture are pumped (Fig. 2), the stored energy in each disk will be 450 J. Here, we took into account the quantum defect and ESA-induced losses of 30% (either by pump ESA or by laser ESA, see above). At the Brewster's angle, the small signal-gain coefficient for each disk will be 1.39 per pass, i.e., 1.93 after reflection (we assumed $E_{spump} = 0.5$ J/cm^2). For the input energy of $W_{in} = 20$ J, the output energy will be 1100 J. After compression with 75% efficiency, the energy of the femtosecond pulse will be 800 J, which corresponds to a 32-PW power for a 25-fs pulse. In these estimations, we assumed $\sigma_{gs} = 70 \times 10^{-19}$ cm^2 for Cr:YAG. The same output parameters can be obtained for only one Cr:YSGG disk. An input energy as small as $W_{in} = 2$ J will be needed, because of the large-gain cross section of Cr:YSGG.

When all four channels of the Luch facility are used, the compressed-pulse power will exceed 100 PW. Note that neither optical breakdown nor self-focusing in ceramic disks limit the output intensity.

6. CONCLUSIONS

The suggested concept of superpowerful femtosecond lasers based on Cr:YAG (or Cr:YSGG) ceramics combines traditional principles (the energy source is nanosecond Nd:glass laser pulses, CPA) with possibilities offered by laser ceramics for new optical materials. Polycrystalline Cr:YAG ceramics simultaneously combine three key properties: a large-gain bandwidth to amplify pulses of up to 20 fs, a wide aperture to amplify chirped pulses up to the multikilojoule level, and a high efficiency of conversion for a narrowband Nd:glass laser pump. These properties open up the opportunity for creating a unique laser with peak powers unattainable by any other techniques.

ACKNOWLEDGMENTS

The authors are grateful for support from the Femtosecond Optics and Novel Laser Materials Program of the Presidium of the Russian Academy of Sciences.

REFERENCES

1. D. M. Pennington, M. D. Perry, B. C. Stuart, et al., in *Proceedings of the Solid State Lasers for Application to Inertial Confinement Fusion: Second Annual International Conference, London, 1997*, Proc. SPIE **3047**, 490–500 (1997).
2. Y. Kitagawa, H. Fujita, R. Kodama, et al., IEEE J. Quantum Electron. **40**, 281–293 (2004).
3. C. N. Danson, P. A. Brummitt, R. J. Clarke, et al., Nucl. Fusion **44**, S239–S246 (2004).
4. M. Aoyama, K. Yamakawa, Y. Akahane, et al., Opt. Lett. **28**, 1594–1596 (2003).
5. V. V. Lozhkarev, G. I. Freidman, V. N. Ginzburg, et al., Laser Phys. Lett. **4**, 421–427 (2007).
6. I. N. Ross, P. Matousek, G. H. C. New, and K. Osvay, J. Opt. Soc. Am. B **19**, 2945–2956 (2002).
7. R. Li, Y. Leng, and Z. Xu, in *Proceedings of the Conference on Lasers and Electro-Optics, 2005*, p. CMB1.
8. J. Hein, S. Podleska, M. Siebold, et al., Appl. Phys. B **79**, 419–422 (2004).
9. C. P. J. Barty, M. Key, J. A. Britten, et al., in *Proceedings of the Conference on Lasers and Electro-Optics, OSA Trends in Optics and Photonics, San Francisco, CA, 2004* (Optical Society of America, Washington, 2004), p. JTuG4.
10. L. J. Waxer, D. N. Maywar, J. H. Kelly, et al., Opt. Photonics News **16**, 30–36 (2005).
11. E. W. Gaul, T. Ditmire, M. D. Martinez, et al., in *Proceedings of the Conference on Lasers and Electro-Optics, Baltimore, 2005*, p. JFB2.
12. N. Blanchot, E. Bignon, H. Coic, et al., in *Proceedings of the Topical Problems of Nonlinear Wave Physics, 2005*, Proc. SPIE **5975**, 0C1-0C16 (2005).
13. J. L. Collier, O. Chekhlov, R. J. Clarke, et al., in *Proceedings of the Conference on Lasers and Electro-Optics, Baltimore, 2005*, p. JFB1.
14. V. V. Lozhkarev, S. G. Garanin, R. R. Gerke, et al., JETP Lett. **82**, 178-180 (2005).
15. J. Li, K.-I. Ueda, H. Yagi, et al., J. Alloys Compd. **341**, 220–225 (2002).

16. J. Kong, D. Y. Tang, J. Li, K. Ueda, et al., Opt. Express **12**, 3560–3566 (2004).
17. Y. Feng, J. Lu, K. Takaichi, et al., Appl. Opt. **43**, 2944–2947 (2004).
18. G. Lin, H. Wei, Z. Hong-bo, et al., Opt. Commun. **13**, 4085–4089 (2005).
19. A. Shirakawa, K. Takaichi, H. Yagi, et al., Opt. Express **11**, 2911–2916 (2003).
20. J. R. Lu, J. Lu, A. Shirakawa, et al., Phys. Status Solidi A **189**, R11–R13 (2002).
21. K. Takaichi, J. R. Lu, T. Murai, et al., Jpn. J. Appl. Phys., Part 2 **41**, L96–L98 (2002).
22. N. B. Angert, N. I. Borodin, V. M. Garmash, et al., Sov. J. Quantum Electron. **18**, 73–74 (1988).
23. E. Sorokin, S. Naumov, and I. T. Sorokina, IEEE J. Sel. Top. Quantum Electron. **11**, 690–712 (2005).
24. P. J. Conlon, J. P. long, P. M. W. French, et al., J. Mod. Opt. **42**, 723–726 (1995).
25. S. Spaelter, M. Boehm, M. Burk, et al., Appl. Phys. B **65**, 335–338 (1997).
26. D. J. Ripin, C. Chudoba, J. T. Gopinath, et al., Opt. Lett. **27**, 61–63 (2002).
27. Z. Burshtein, P. Blau, Y. Kalisky, et al., IEEE J. Quantum Electron. **34**, 292–299 (1998).
28. H. Eilers, U. Hommerich, S. M. Jacobsen, et al., Phys. Rev. B **49**, 505-515, 513 (1994).
29. H. Eilers, K. R. Hoffman, W. M. Dennis, et al., Appl. Phys. Lett. **61**, 2958–2960 (1992).
30. N. I. Borodin, V. F. Zhitnyuk, A. G. Okhrimchuk, and A. V. Shestakov, Izv. Akad. Nauk USSR, Ser. Fiz. **54**, 1500-1506 (1990).
31. A. G. Okhrimchuk and A. V. Shestakov, Opt. Mater. **3**, 1–13 (1994).
32. P. M. W. French, N. H. Rizvi, J. R. Taylor, and A. V. Shestakov, Opt. Lett. **18**, 39–41 (1993).
33. A. G. Okhrimchuk and A. V. Shestakov, Phys. Rev. B **61**, 988–995 (2000).
34. K. Spariosu, W. Chen, R. Stultz, et al., Opt. Lett. **18**, 814 (1993).
35. S. Camacho-Lopez, R. P. M. Green, G. J. Crofts, and M. J. Damzen, J. Mod. Opt. **44**, 209–219 (1997).
36. Y. Shimony, Z. Burshtein, and Y. Kalisky, IEEE J. Quantum Electron. **31**, 1738 (1995).
37. S. Kuck, K. Petermann, U. Pohlmann, and G. Huber, Phys. Rev. B: Condens. Matter. **51**, 17323–17331 (1995).
38. S. Kuck, Appl. Phys. B **72**, 515–562 (2001).
39. V. Kartazaev and R. R. Alfano, Opt. Commun. **242**, 605–611 (2004).
40. A. Sennaroglu, C. R. Pollock, and H. Nathel, J. Opt. Soc. Am. B **12**, 930 (1995).
41. V. V. Lozhkarev, G. I. Freidman, V. N. Ginzburg, et al., Laser Phys. **15**, 1319–1333 (2005).
42. A. Dement'ev and R. Navakas, Nonlinear Anal.: Model. Control **6**, 39–55 (2001).
43. M. A. Jaspan, D. Welford, and J. A. Russell, Appl. Opt. **43**, 2555–2560 (2004).
44. N. N. Il'ichev, A. V. Kir'yanov, and P. P. Pashinin, Quantum Electron. **28**, 147–151 (1998).
45. L. M. Frantz and J. S. Nodvik, Appl. Phys. **34**, 2346 (1963).
46. A. V. Kir'yanov and C. G. Bermudez, J. Opt. Soc. Am. B **20**, 2454–2469 (2003).
47. S. Kuck, K. L. Schepler, S. Hartung, et al., J. Lumin. **72–74**, 222–223 (1997).
48. S. G. Garanin, A. I. Zaretskii, R. I. Il'kaev, et al., Quantum Electron. **35**, 299–301 (2005).

SPELL: 1. careated